Mausam, (1995), **46**, 4, 435-444

550.34.016

A study of aftershocks of 20 October 1991 Uttarkashi earthquake

R. S. DATTATRAYAM*
Department of Science & Technology, New Delhi
and
V. P. KAMBLE
India Meteorological Department, New Delhi
(Received 25 July 1994, Modified 3 February 1995)

सार — 20 अक्तूबर 1991 के उत्तरकाशी भूकम्प से गढ़वाल हिमालय क्षेत्र में बड़े पैमाने पर क्षति हुई। इसके उपरांत दो महीने तक भूकम्प के बाद के झटके महसूस किए गए। मुख्य भूकम्प के उपरांत स्थापित किए गए अस्थायी नेटवर्क से और उस क्षेत्र में कार्य कर रहे स्थायी केन्द्रों के उपयोग से भूकम्प के बाद के झटकों का मॉनीटरन किया गया। इन केन्द्रों के आंकड़ों के उपयोग से भूकम्प के बाद के लगभग 142 झटकों का पता लगाया गया। भूकम्प के बाद के झटकों (उत्तरघात) की शृंखला के लिए गुटेनबर्ग-रिक्टर संबंध की बी-वेल्यू 0.6 बैठती है। भूकम्प के बाद के झटकों का कालिक वितरण 1.17 के स्थिर क्षय (पी) के साथ अति परवलयिक क्षय दर्शाता है। फ़ील्ड-सर्वेक्षण से प्राप्त सूक्ष्म भूकम्पीय प्रेक्षणों की सूचना अन्य यंत्रों के माध्यम से प्राप्त सूचना से काफ़ी मेल खाती है।

ABSTRACT. The Uttarkashi earthquake of 20 October 1991, which caused widespread damage in the Garhwal Himalayan region, was followed by a prominent aftershock activity extending over a period of about two months. The aftershock activity was monitored using temporary networks established after the mainshock and the permanent stations in operation in the region. About 142 aftershocks could be located accurately using the data of these stations. The b-value of the Gutenberg-Richter's relationship for the aftershock sequence works out to be 0.6. The temporal distribution of the aftershocks suggests a hyperbolic decay with a decay constant (p) of 1.17. Macroseismic observations derived from field surveys show good agreement with the instrumentally determined source parameters.

Key words — Aftershock, Magnitude, Mainshock, Main Central Thrust (MCT), Energy, Fault length.

1. Introduction

A moderate, but destructive earthquake of body-wave magnitude 6.6 occurred in the early hours of 20 October 1991 which caused widespread damage to property and structures and left 768 people killed in the Garhwal Himalayan region. The earthquake has caused extensive landslides and ground fissures in the Bhagirathi and Bhilangana valleys although no evidence of surface faulting was found in the field (Narula and Shome 1992). Among the engineering structures which suffered major damage was an iron-span bridge at village Gawana about 8 km from Uttarkashi.

Seismic activity in this region is mostly ascribed to several thrust planes running parallel to the Himalayas, *viz.*, the Indus Suture Zone (ISZ), Main Central Thrust (MCT), Main Boundary Thrust (MBT) and Main Frontal Thrust (MFT) and other transcurrent features. These tectonic features, in turn, are the manifestations of the processes related to northward movement of Indian plate with respect to Eurasian plate. This earthquake with its epicentre located east of Uttarkashi is very close to MCT and the fault plane solution of USGS suggests a predominant reverse faulting on a NW-SE trending plane dipping in northeast direction.

The mainshock was preceded by two foreshocks and followed by a number of aftershocks over a period of about two months. The largest one with a magnitude of 5.2 (M_L) occurred just eight hours after the main event. On the very first day, eight aftershocks strongly jolted the nearby areas sending the local population flee outdoors. While few aftershocks widened the old cracks and caused fresh ones in houses and other buildings, some of them even caused damage to those structures which were badly affected by the mainshock. The paper presents a detailed analysis of the aftershocks that followed the mainshock.

2. Monitoring of aftershock activity

The aftershock activity is monitored by the temporary networks set up by India Meteorological Department (IMD), Geological Survey of India

* Views expressed in this paper are of the author only and do not reflect those of the organisation he is working for.

TABLE 1

Location of seismic stations

S. No.	Station	Lat. (°N)		Long. (°E)		Elevation (m)	Period of operation (1991)	Organisation
		deg.	min	deg	min			
				Temporary Network				
1.	Chinyali-Saur (CHL)	30	34.43	78	19.49	1000	29-30 Oct 3 Nov-4 Dec	NGRI GSI
2.	Uttarkashi (UTK)	30 30	43.62 43.68	78 78	26.81 27.00	1109	30 Oct-13 Nov 21 Nov-10 Dec	NGRI IMD
3.	Barkot (BAK)	30	48.41	78	11.89	1200	4-15 Nov	GSI
4.	Bhatwari (BTW)	30	48.60	78	36.60	1600	5 Nov-5 Dec 21 Nov-12 Dec	GSI IMD
5.	Ghansali (GHL)	30	27.24	78	38.76	950	16 Nov-4 Dec	GSI
6.	Ghuttu (GTU)	30	31.81	78	47.52	1600	25 Nov-4 Dec	GSI
7.	Tehri (TEH)	30	22.80	78	29.40	—	17 Nov-9 Dec	IMD
				Permanent Stations of IMD				
8.	Dehradun (DDN)	30	19.00	78	03.00	682	—	—
9.	Shimla (SML)	30	07.00	77	10.00	—	—	—
10.	Dalhousie (DLH)	35	32.50	75	58.00	—	—	—
11.	Dharamsala (DHM)	32	13.00	76	20.00	—	—	—

(GSI) and National Geophysical Research Institute (NGRI), Hyderabad in addition to the permanent observatories maintained in the region by IMD and Wadia Institute of Himalayan Geology (WIHG), Dehradun. A list of temporary and permanent seismic stations togetherwith their location and period of observation, operated by various departments/ organisations, is given in Table 1. It includes only those stations whose data has been used in the estimation of hypocentral parameters of aftershocks. The temporary seismic stations set up in the region are also shown in Fig. 1. It may be seen that the number of seismic stations set up and the duration of operation was not uniform over the period of observation. This has resulted in varying levels of detection and location capabilities of the network over different periods of observation. For example, the number of located events during the first fortnight is much less than the actual activity, as the events could be located using the data of distant permanent stations only. Similarly, the number of located events is more during the period when closely spaced stations were in operation during November and early part of December. The aftershock data is analysed by GSI for the period 12 November to 4 December 1991 and by IMD for the rest of the period. Hypocentral parameters of all the events are determined using localization programme HYPO-71. A three layered velocity model, as given below, is used in estimating the hypocentral locations.

Layer thickness (km)	*P-wave velocity* (km/sec)
0 — 24	5.72
24 — 45	6.61
>45	8.22

$(V_p/V_s = 1.74)$

A minimum of three *P*-arrivals and two *S*-arrival times are used for locating these events. For larger aftershocks, magnitude (M_L) as measured from Wood-Anderson seismograph is used wherever

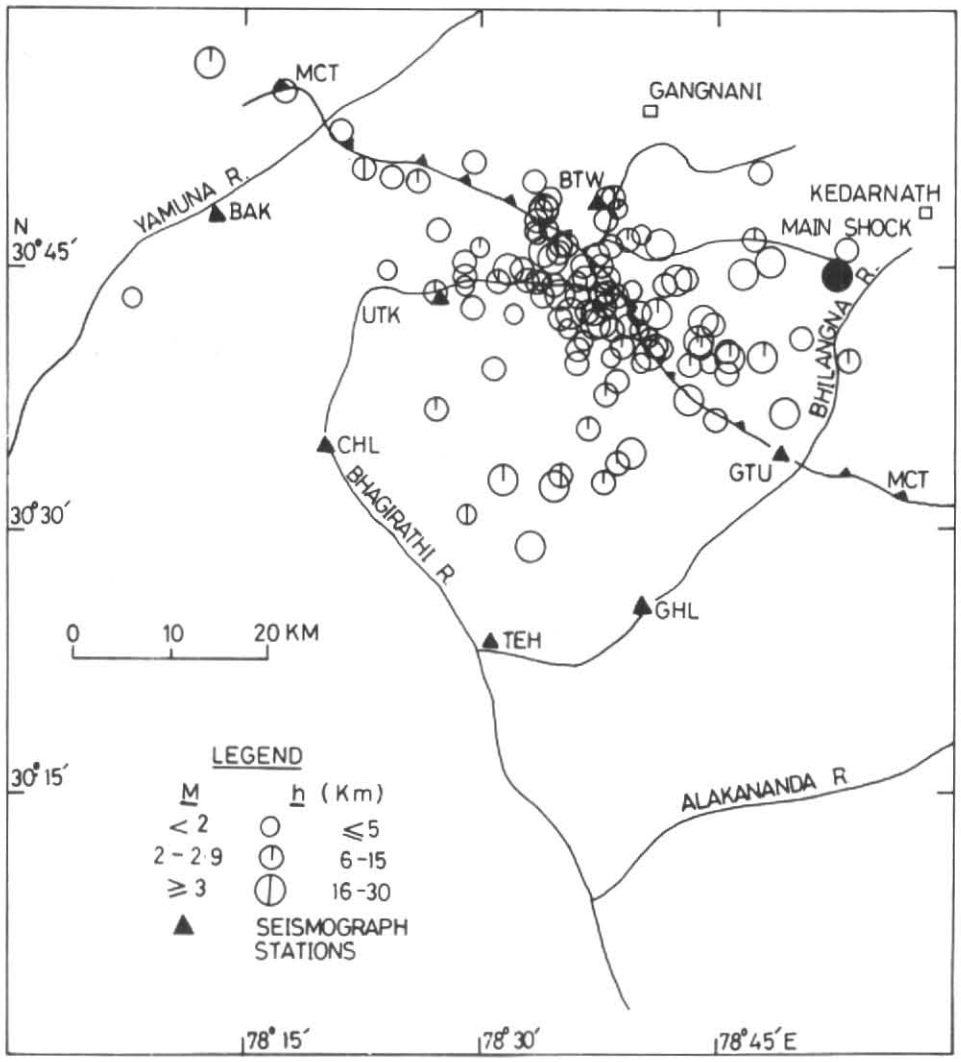

Fig. 1. Map showing the locations of temporary seismograph stations, mainshock, aftershocks and surface trace of MCT

available. Magnitudes of smaller events are estimated using the following empirical formula,

$$M_D = -2.44 + 2.61 \log D \qquad (1)$$

where "M_D" is the duration magnitude and "D" is the signal duration in seconds. Duration magnitudes estimated by IMD for the month of October 1991 are based on the formula given below :

$$M_D = -0.87 + 2 \log D + 0.0035 R \qquad (2)$$

where "R" is the epicentral distance in km.

The list of aftershocks compiled by Kayal *et al.* (1992) is updated and the locations of 142 aftershocks are given in Table 2.

The time residuals (RMS) and the errors in the location of epicentre (ERH) and focal depth (ERZ) are within 0.5 sec., 5 km and 5 km respectively for most of the events.

3. Data analysis and discussion

Fig. 1 depicts the locations of seismograph stations, mainshock, aftershocks and surface trace

TABLE 2

Hypocentral parameters of aftershocks

Date YM D	Origin time (UTC)			Lat.°N		Long°E		Depth (km)	Mag. (M_D)	No.	RMS (sec)	ERH (km)	ERZ (km)
	H	M	S	deg	min	deg	min						
911019	22	04	17.74	30	46.27	78	41.60	4.28	*3.4	16	0.68	3.6	3.3
911019	22	08	17.27	30	37.84	78	38.03	12.51	*2.4	14	0.73	3.7	3.0
911019	22	29	20.59	30	37.38	78	42.90	0.71	*4.0	23	1.76	5.1	4.8
911019	22	41	18.26	30	40.23	78	40.70	15.00	*4.7	19	1.94	8.7	7.7
911019	22	56	21.56	30	41.90	78	44.05	1.29	*4.0	11	1.04	7.1	5.0
911019	23	10	6.94	30	43.03	78	40.93	12.08	—	15	1.50	6.9	3.5
911019	23	39	30.35	30	42.26	78	41.26	12.03	*3.5	18	1.26	8.0	4.7
911020	01	04	26.77	30	41.59	78	48.25	11.79	—	15	0.88	4.6	3.9
911020	01	13	13.35	30	50.60	78	47.36	2.07	*2.4	16	1.42	6.7	4.4
911020	01	21	2.04	30	44.53	78	36.32	8.64	*2.3	21	1.60	6.5	4.5
911020	01	24	59.83	30	39.86	78	47.78	6.89	*4.2	20	1.73	6.3	4.8
911020	03	34	29.21	30	46.00	78	53.23	1.10	*2.9	22	1.68	5.7	4.5
911020	04	20	27.87	30	43.57	78	37.85	5.56	*3.0	27	1.36	4.8	3.2
911020	04	31	30.28	30	40.87	78	43.72	8.82	*3.5	15	1.25	5.4	4.8
911020	05	32	27.58	30	43.93	78	37.85	2.01	*5.2	34	1.38	4.9	3.2
911020	05	54	42.83	30	52.21	78	45.27	3.14	—	8	0.71	6.6	4.3
911020	05	57	30.38	30	52.26	78	39.39	3.55	—	8	0.48	4.3	2.9
911020	06	48	7.67	30	45.05	78	31.57	2.62	3.1	24	1.57	6.2	4.8
911020	07	25	49.58	30	35.82	78	36.70	15.00	2.9	15	1.65	7.7	7.0
911020	07	56	31.54	30	39.90	78	45.65	11.45	3.5	29	1.50	5.9	4.5
911020	09	01	5.95	30	32.85	78	35.07	20.95	2.7	11	1.07	6.2	7.4
911020	09	45	5.10	30	45.78	78	37.24	1.91	2.7	9	0.66	4.2	4.0
911020	10	17	56.61	30	44.65	78	37.58	1.57	2.7	12	1.12	5.0	4.1
911020	10	39	22.07	30	44.35	78	30.90	6.74	2.6	8	1.23	12.6	7.8
911020	11	10	29.15	30	43.50	78	38.53	9.47	2.7	11	1.04	6.3	5.4
911020	21	48	47.65	30	44.20	78	42.82	1.79	2.4	9	0.87	5.5	5.6
911020	23	58	37.90	30	46.40	78	34.88	1.52	2.7	7	1.04	12.7	7.2
911021	14	02	44.32	30	45.47	78	48.21	1.82	*3.6	19	1.51	8.3	4.8
911021	14	28	12.17	30	47.84	78	33.42	3.28	2.6	10	1.58	9.8	6.7
911021	14	36	3.08	30	47.26	78	27.23	3.83	2.6	13	1.24	8.0	4.8
911021	18	44	11.54	30	47.93	78	37.98	0.25	2.5	8	0.70	6.9	4.7
911021	22	32	4.55	30	43.89	78	41.41	4.05	2.8	8	0.64	6.8	4.7
911022	06	39	26.60	30	49.23	78	34.23	0.43	2.7	15	0.99	4.0	4.0
911022	11	15	32.75	30	48.61	78	34.01	5.21	*3.4	12	0.44	2.9	1.8
911024	00	04	46.60	30	48.46	78	33.73	4.39	2.5	13	0.81	3.6	2.8
911024	08	11	21.45	30	44.11	78	37.25	0.03	*3.2	10	0.57	4.7	3.2
911024	19	21	0.02	30	43.40	78	35.50	2.92	*3.5	19	1.46	5.0	4.0
911024	20	40	4.00	30	43.73	78	26.93	11.78	2.5	8	0.93	9.9	5.5

TABLE 2 (*contd.*)

Date YMD	Origin time (UTC)			Lat.°N		Long°E		Depth (km)	Mag. (M_D)	No.	RMS (sec)	ERH (km)	ERZ (km)
	H	M	S	deg	min	deg	min						
911025	15	22	43.44	30	46.24	78	38.28	1.57	2.9	9	1.17	10.4	6.4
911025	19	09	22.53	30	50.19	78	33.29	0.12	2.7	8	1.02	13.3	6.1
911027	00	40	24.16	30	44.57	78	46.64	3.72	*4.1	13	1.25	6.0	3.9
911027	13	19	40.54	30	44.36	78	42.43	3.27	*4.0	12	1.82	14.1	8.7
911027	19	29	38.31	30	46.74	78	47.17	15.00	2.7	7	1.37	14.9	—
911111	19	43	44.71	30	51.10	78	22.64	26.48	2.38	6	.40	5.8	8.6
911111	20	43	47.83	30	43.98	78	34.30	7.48	2.11	6	.16	2.1	4.6
911111	21	01	24.62	30	43.42	78	08.01	0.86	1.85	5	.08	1.6	—
911111	21	35	13.66	30	53.21	78	21.10	1.94	2.05	6	.22	2.1	—
911112	05	03	01.79	30	44.59	78	38.01	0.88	1.89	5	.29	1.1	7.4
911112	20	28	52.69	30	38.72	78	38.56	1.60	1.97	5	.53	7.1	—
911112	23	50	12.26	30	43.03	78	37.13	0.59	2.66	6	.07	1.1	—
911113	00	31	34.27	30	41.58	78	38.32	7.82	2.76	6	.17	2.7	5.1
911113	01	06	13.81	30	42.39	78	39.86	1.10	2.55	5	.18	2.0	—
911113	12	11	13.87	30	45.10	78	32.43	1.34	2.86	5	.31	2.7	—
911113	18	35	00.76	30	42.13	78	36.15	0.31	2.73	6	.14	1.9	—
911114	00	04	27.94	30	36.65	78	49.21	0.50	3.16	6	.30	3.4	—
911114	07	44	38.03	30	42.25	78	35.13	6.11	1.99	6	.18	2.6	6.8
911114	10	32	09.89	30	43.47	78	36.09	1.17	2.32	6	.20	1.1	—
911114	17	31	57.33	30	33.78	78	38.73	11.27	2.61	6	.09	1.6	3.2
911114	17	35	38.85	30	44.36	78	33.58	1.07	2.02	6	.10	1.1	—
911114	18	26	14.09	30	40.47	78	41.02	2.16	2.29	6	.12	2.0	—
911114	19	52	28.42	30	40.81	78	36.62	1.41	1.49	6	.19	1.8	—
911114	20	36	01.94	30	43.46	78	38.20	1.15	1.44	6	.91	9.4	—
911114	22	53	16.77	30	43.41	78	35.20	1.17	1.55	6	.08	0.9	—
911115	03	44	42.51	30	40.07	78	45.56	0.99	2.58	6	.14	2.4	—
911115	12	11	21.84	30	41.59	78	39.91	1.41	1.88	6	.37	2.0	—
911115	13	09	16.33	30	45.15	78	36.58	10.37	2.43	5	.04	0.9	1.3
911115	15	39	14.39	30	41.89	78	37.08	5.58	3.19	6	.07	1.0	2.6
911115	18	30	57.92	30	41.74	78	35.42	2.45	1.04	6	.16	0.4	2.6
911115	20	43	39.22	30	30.75	78	29.22	15.90	1.50	5	.34	9.2	—
911116	01	04	46.45	30	34.46	78	39.39	1.37	2.95	6	.10	0.9	—
911117	13	32	07.78	30	44.55	78	35.98	1.39	1.76	6	.14	1.8	—
911117	18	44	50.59	30	45.00	78	37.43	7.84	2.79	5	.12	2.8	5.4
911118	00	19	17.79	30	44.05	78	33.48	0.37	2.10	5	.08	1.4	—
911118	03	22	22.62	30	43.14	78	37.97	1.08	2.35	6	.05	0.4	6.2
911118	15	18	14.82	30	42.37	78	35.48	1.08	3.01	5	.02	0.1	1.4
911118	16	09	55.20	30	55.65	78	17.31	0.89	2.17	6	.46	8.1	—
911119	12	03	17.47	30	45.94	78	33.87	2.12	3.05	5	.34	3.7	—
911119	14	38	06.66	30	43.20	78	35.62	10.46	2.90	6	.28	3.1	7.0
911119	15	11	58.67	30	45.93	78	36.67	11.61	1.55	6	.12	1.6	2.2
911119	19	43	33.40	30	46.07	78	34.93	2.91	2.57	6	.20	2.7	10.0
911119	21	50	06.81	30	50.59	78	24.40	1.16	2.14	5	.23	3.5	—
911120	03	02	26.79	30	44.18	78	33.98	0.93	1.95	6	.09	0.6	—
911120	15	47	28.89	30	42.42	78	36.81	8.55	2.08	6	.11	1.2	3.3

TABLE 2 (*contd.*)

Date YMD	Origin time (UTC)			Lat.°N		Long°E		Depth (km)	Mag. (M_D)	No.	RMS (sec)	ERH (km)	ERZ (km)
	H	M	S	deg	min	deg	min						
911120	16	14	56.45	30	29.11	78	33.10	1.34	3.06	5	.20	0.9	—
911120	19	50	06.97	30	41.76	78	44.59	0.85	2.06	6	.43	4.9	—
911121	01	03	03.27	30	40.41	78	36.15	0.97	2.28	6	.12	1.0	—
911121	07	52	35.72	30	46.19	78	29.88	7.01	0.04	6	.18	2.2	5.8
911121	15	48	35.37	30	42.09	78	36.85	0.08	1.55	6	.29	1.2	—
911121	19	54	03.62	30	49.49	78	38.48	9.27	2.14	6	.09	1.6	1.2
911122	15	52	24.21	30	43.55	78	37.79	15.13	2.98	8	.24	2.1	3.3
911122	20	48	29.95	30	39.72	78	40.16	1.04	1.14	6	.06	0.4	9.7
911123	04	52	07.47	30	42.73	78	36.63	6.14	3.13	7	.25	2.1	8.7
911123	18	45	26.28	30	44.78	78	28.92	0.28	1.98	6	.13	1.4	—
911123	18	46	02.44	30	44.14	78	28.77	1.32	1.45	6	.21	2.1	—
911123	18	53	39.20	30	39.09	78	45.51	1.19	2.25	6	.29	0.9	—
911123	19	18	30.12	30	41.05	78	40.51	12.14	1.19	6	.09	1.0	2.2
911123	19	52	44.44	30	42.57	78	32.08	1.06	1.32	6	.30	1.5	—
911123	20	35	03.83	30	45.74	78	36.56	0.31	1.55	6	.26	3.7	—
911123	21	22	07.49	30	42.45	78	36.71	1.53	1.59	6	.08	0.2	2.6
911124	01	02	47.15	30	40.68	78	38.75	9.60	2.62	6	.31	3.3	9.2
911124	06	18	40.24	30	43.27	78	39.65	5.51	—	6	.16	1.9	6.2
911124	13	19	40.31	30	45.59	78	28.77	0.86	2.81	6	.05	0.3	7.4
911124	23	31	09.48	30	40.06	78	38.34	0.23	1.36	6	.28	2.7	—
911125	14	29	49.89	30	41.76	78	37.68	0.34	3.72	8	.29	1.9	—
911125	18	59	47.40	30	43.64	78	35.05	2.69	3.49	6	.35	1.7	—
911125	19	36	13.80	30	51.41	78	29.64	1.19	2.42	6	.34	1.6	—
911125	21	31	01.96	30	43.48	78	36.73	2.02	1.18	6	.49	5.0	—
911126	07	02	16.33	30	40.55	78	41.49	14.95	2.35	8	.76	6.5	—
911126	08	21	44.42	30	43.05	78	37.95	10.44	1.80	6	.06	0.7	1.5
911126	10	32	25.37	30	46.84	78	39.26	9.18	2.47	8	.19	1.9	2.4
911126	18	01	17.46	30	45.06	78	24.07	1.13	0.48	6	.37	2.8	—
911128	05	01	28.12	30	50.23	78	25.92	7.68	2.78	8	.21	2.4	3.2
911128	22	13	26.68	30	45.68	78	34.51	0.60	3.28	8	.25	2.2	—
911129	01	53	04.70	30	47.25	78	33.27	10.46	1.40	6	.28	3.8	5.6
911129	23	47	46.01	30	39.72	78	35.76	0.30	2.61	6	.14	1.2	—
911130	00	09	20.27	30	47.56	78	34.50	0.70	1.78	6	.23	3.4	—
911130	12	20	26.34	30	44.56	78	32.45	10.12	2.24	8	.03	0.2	0.4
911130	13	01	50.54	30	43.51	78	33.89	0.72	2.39	6	.10	0.8	—
911130	21	22	32.38	30	39.32	78	30.66	1.36	2.03	6	.23	0.3	8.3
911130	21	29	16.68	30	43.65	78	39.64	1.24	1.38	6	.09	1.1	—
911201	15	18	07.44	30	47.04	78	40.24	12.81	1.66	6	.10	1.5	1.6
911201	16	02	36.31	30	39.69	78	53.10	5.43	2.04	5	1.71	14.4	—
911201	16	19	11.27	30	43.46	78	37.75	1.20	1.46	6	.07	0.6	8.6
911203	03	04	51.47	30	46.50	78	35.26	6.24	2.25	6	.06	0.8	1.5

TABLE 2 (*contd.*)

Date YMD	Origin time (UTC)			Lat.°N		Long°E		Depth (km)	Mag. (M_D)	No.	RMS (sec)	ERH (km)	ERZ (km)
	H	M	S	deg	min	deg	min						
911203	01	36	27.21	30	48.70	78	38.76	10.14	2.02	6	.19	2.6	2.1
911203	06	04	32.19	30	37.01	78	27.10	8.87	2.20	6	0.63	8.5	—
911203	18	54	33.17	30	40.95	78	50.15	3.30	1.95	7	0.97	2.7	6.6
911205	00	01	6.39	30	40.60	78	43.82	9.46	1.96	6	0.18	2.3	5.7
911205	03	12	46.56	30	39.38	78	43.26	10.95	2.19	6	0.04	0.6	0.3
911206	11	31	43.29	30	48.70	78	34.07	8.54	2.42	8	0.49	4.2	2.6
911207	00	13	38.12	30	42.87	78	37.90	3.96	1.76	6	0.19	1.4	6.1
911207	01	08	4.33	30	47.07	78	33.46	6.01	1.81	6	0.25	1.1	1.7
911207	17	16	18.68	30	41.70	78	39.44	15.00	2.14	7	0.40	3.7	2.3
911208	15	46	31.79	30	42.64	78	36.70	10.25	3.17	13	0.91	5.0	2.3
911228	17	27	21.97	30	43.74	78	34.77	3.74	2.8	15	1.08	6.6	4.2
920213	20	23	05.34	30	39.64	78	44.38	1.68	1.9	15	0.94	5.9	3.8
920302	14	48	21.33	30	32.77	78	31.44	15.00	3.4	16	1.76	10.4	7.1
920314	12	40	27.49	30	32.22	78	34.78	1.77	4.9	11	0.83	6.6	4.9
920315	03	15	30.43	30	36.40	78	44.65	0.15	2.8	14	0.97	5.9	4.3
920422	06	08	46.71	30	57.40	78	12.70	7.04	3.8	15	1.72	10.9	6.2
920516	08	41	07.78	30	32.39	78	37.74	8.48	2.7	15	1.31	8.0	5.8
920630	13	06	49.91	30	42.86	78	29.51	3.52	2.6	8	0.81	5.8	3.3

Y — Year
M — Month
D — Day
H — Hour
M — Minute
S — Second

M_D — Duration magnitude
RMS — Root Mean Square
ERH — Location error in epicentre
ERZ — Error in focal depth
• — Richter magnitude

of MCT. The aftershock activity defines a zone of 30 × 40 sq km extending in NW-SE direction and the mainshock is located on the eastern margin of this zone. It has been observed in the past by various workers that the mainshock usually falls on the periphery of the aftershock zone and the area bounded by the aftershocks defines the source dimensions of the mainshock. The largest aftershock of magnitude 5.2 (M_L) occurred at the centre of this zone. According to Bath's law, the difference in magnitude between the mainshock and the largest aftershock is roughly 1.2, which is 1.0 in the present case. The mainshock and the aftershocks are located close to the surface trace of MCT and may be related to it, indicating that MCT is active. The shallower shocks, particularly those which are located south of MCT, may be associated with smaller thrusts or faults genetically related to MCT.

While the focal depth of the mainshock is estimated as 12 km, majority of the aftershocks have focal depths varying between 0-15 km with few exceeding 15 km. About 62% of the events occurred within the top layer of 5 km thickness, 36% between 6 and 15 km and only 2% in the depth range of 16-30 km. Thus, the foci of the aftershocks lay mostly within 15 km below the surface. Although the depth-wise distribution of aftershocks does not indicate any clear trend, it is observed that the deeper and larger magnitude events are mostly concentrated along a NE-SW trending plane southeast of the shallow cluster of events. The available data set with regard to focal depth resolution, does not, however, permit any further inference on the likely fault plane of the mainshock. The fault plane solution for the mainshock, as given by USGS, however indicates a shallow northeast dipping, northwest-southeast trending nodal plane with predominant reverse type of faulting.

The magnitude-wise distribution of aftershocks reveals that one aftershock is of magnitude greater than 5 and seven are of magnitude between 4 and 5.

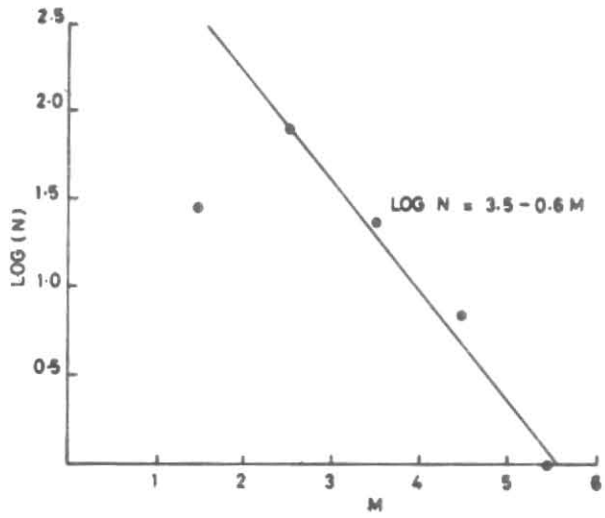

Fig. 2. Frequency-magnitude plot of aftershocks

The frequency-magnitude plot for the aftershock sequence is shown in Fig. 2. It may be seen that the number of events reported for magnitudes less than about 2.0 is considerably less than that predicted by the Gutenberg-Richter's frequency-magnitude relation. A least-square fit of the whole data sets yields lower estimates of '*a*' and '*b*' as 2.5 and 0.4 as against 3.5 and 0.6 respectively for the data set with $M > 2.0$, which is in good agreement with the estimates obtained by Gibowicz (1973) for aftershock sequences in California and New Zealand regions.

Seismic wave energy is an important parameter used to quantify the strength of an earthquake and may be estimated using the empirical formula (Richter 1958),

$$\log E = 5.8 + 2.4\, M_b \qquad (3)$$

For the mainshock, seismic wave energy works out to 4.37* — 10**21 ergs. However, for the aftershocks, energy is computed from M_L, using the following relationship (Richter 1958),

$$\log E = 9.9 + 1.9\, M_L - 0.024\, M_L^2 \qquad (4)$$

The energy release in the largest aftershock (M_L = 5.2) is estimated as 1.35* 10** 19 ergs and the same for the aftershocks during the first week (excluding the largest aftershock) works out to be 0.30* 10** 19 ergs. The energy released in the rest of the aftershock sequence is about 0.45* 10** 19 ergs. The energy released in the entire aftershock sequence is about half the energy released in the largest aftershock and about two orders less than that of the mainshock.

Temporal distribution of aftershocks is studied using the data of Shimla (SML) for which a more or less complete data set is available. Fig. 3 is a histogram showing the number of events recorded at SML, with the highest number of 80 events recorded on 20 October 1991. On subsequent days, the frequency of aftershocks dropped to 38 and 20 respectively and within a week the average dropped to 5 to 6 shocks per day. The decay pattern of aftershocks is usually expressed by the well known relationship after Utsu (1961), according to which, the activity decays hyperbolically with time,

$$N(t) = At^{-p} \qquad (5)$$

where $N(t)$ is the number of aftershocks after time "t" and "A" and "p" are constants. The constant "A" determines the level of activity and "p" determines the decay rate. Normally "p" takes a value close to 1. The aftershock data of SML fits the following relationship, obtained by least-squares method :

$$N(t) = 83^* t^{-1.17} \qquad (6)$$

The unit time interval is taken as 1 day in deriving the above relationship. Srivastava and Kamble (1972) reported decay constants varying between 1.27 and 1.49 for five earthquakes in the Himalayan region, which show good agreement with the aftershock decay pattern of Uttarkashi earthquake.

Macroseismic observations obtained from direct field studies are of great importance in supplementing the instrumentally recorded quantities. Field investigations carried out by GSI indicated that the maximum intensity of IX is confined to a localised area in a linear tract (Narula and Shome 1992). The peak ground acceleration recorded by the strong motion instruments at Bhatwari and Uttarkashi are of the order of 30% g (Chandrasekharan and Das 1991). A Number of workers have attempted to empirically relate maximum intensity (I_o), ground acceleration (a_o), seismic wave energy and magnitude. The recorded peak ground acceleration of 30% g at Bhatwari and Uttarkashi is in good agreement with the following relationship between maximum intensity and ground acceleration proposed by Richter (1958) :

$$I_o = 3 \log a_o + 1.5 \qquad (7)$$

The following empirical relationship (Karnik 1965) also predicts a maximum intensity of IX for an earthquake of magnitude M_S = 7.1 (USGS),

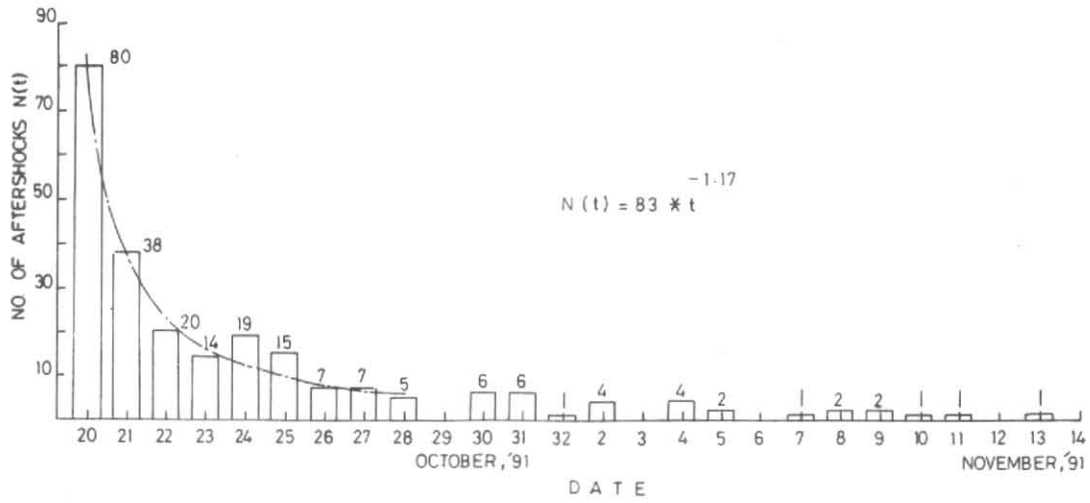

Fig. 3. Histogram showing the number of aftershocks recorded at Shimla (SML) observatory

$$M_s = 2/3^* I_o + 1$$

Fault length (L) may be estimated from earthquake magnitude, as proposed by Press (1975) and Rastogi (1987) respectively :

$$\log L = 0.62\, M_s + 2.19 \quad \text{(L in cm)} \qquad (8)$$

$$\log L = 0.35\, M_b - 0.68 \quad \text{(L in km)} \qquad (9)$$

where "L" is fault length. The fault length as estimated from the long axis of the aftershock area is about 40 km and shows good agreement with the above relationships.

Fault dislocation (D) may be obtained from seismic moment (M_o) and fault area (A), as suggested by Aki (1966),

$$M_o = \mu A\, D \qquad (10)$$

where, M_o—seismic moment, A—fault area and μ—rigidity of the medium.

For M_o = 1.8* 10** 26 dyne cm. (USGS)

A = 1200 sq km

and μ = 3.3* 10** 11 dyne/cm^2,

the dislocation works out to be 46 cm. For a circular fault of radius 20 km [$r = (A/\pi)^{1/2}$], the stress drop ($\Delta\sigma$) works out to be 10 bars from the relation (Kanamori and Anderson 1975) :

$$\text{Stress drop } (\Delta\sigma) = \frac{7\pi}{16} \quad \frac{\mu D}{r} \qquad (11)$$

Gibowicz (1973) studied eighteen aftershock sequences from California and New Zealand regions and found that the stress drop in the main earthquake determines the principal characteristics of the aftershock sequences. A low stress drop leads to a low value of the coefficient "b", high magnitude of the largest aftershock and short duration and conversely. For the set of earthquake sequences studied, he obtained a linear relationship between M_L and log $\Delta\sigma$, according to which a stress drop of 10 bars characterises a shock of M_L = 6.5, showing good agreement with the present estimates. Dynamic source parameters, *viz.*, seismic moment, source radius and stress drop of some foreshocks and aftershocks of Uttarkashi earthquake have been worked out by Dattatrayam *et al.* (1995) using the *P*-wave displacement spectra. They have found that the stress drop in the Uttarkashi earthquake sequence decreased from about 10 bars in the mainshock to about 1.7–4.4 bars in the aftershocks.

4. Conclusions

The aftershock activity that followed the 20 October 1991 Uttarkashi earthquake, continued for over a period of about two months and was monitored by permanent as well as temporary networks operated by various departments/organisations. The aftershock activity defines an elliptical zone of about 40 × 30 sq km extending in a NW-SE direction. While the mainshock is located on the eastern edge of this zone, the largest aftershock of magnitude 5.2 (M_L), which occurred just eight hours after the mainshock, falls in the centre of this zone. The mainshock and the aftershocks are located

close to the surface trace of MCT and may be related to it. The energy released in the entire aftershock sequence is estimated as 0.75* 10** 19 ergs and is about half the energy released in the largest aftershock. The energy released in the mainshock is, however, two orders higher than that of the entire aftershock sequence including the largest aftershock. The focal depths of the mainshock and the aftershocks lie mostly between near surface and 15 km and majority of them are confined to the top layer of 5 km thickness. The deeper and larger magnitude events are mostly concentrated along a NE-SW trending plane southeast of the shallow cluster of events. However, the available aftershock data does not permit any further inference on the likely fault plane of the mainshock. The difference in magnitude between the mainshock and the largest aftershock is 1.0 and follows the Bath's law approximately. The *b*-value of the Gutenber-Richter's relationship for the aftershock sequence works out to be 0.6. The decay pattern of aftershock activity at Shimla (SML), for which a more or less complete data set is available, suggests a hyperbolic decline with time with a decay constant of 1.17, in agreement with the relationship of Utsu (1961) and the decay constants obtained for five other Himalayan earthquakes (Srivastava and Kamble 1972). Macroseismic observations obtained from field investigations show good agreement with several instrumentally determined parameters in accordance with various standard empirical formula.

Acknowledgements

One of the authors, R. S. Dattatrayam, is grateful to the Secretary, Department of Science and Technology, New Delhi for encouragement. The authors are also thankful to the Director General of Meteorology for permission to publish the paper.

References

Aki, K., 1966, "Generation and propagation of G-waves from the Niigata earthquake of June 16, 1964. Part. 2. Estimation of earthquake moment, released energy and stress-strain drop from the G-wave spectrum," *Bull. Earth. Res. Instt.*, **44**, 73-78.

Chandrasekharan, A. R. and Das, J., 1991 "Analysis of strong motion accelerographs of Uttarkashi earthquake of Oct. 20, 1991", Earthquake Engineering Studies Report No. EQ : 91-10, University of Roorkee, Roorkee.

Dattatrayam, R. S., Kamble, V. P. and Srivastava, H. N., 1995, "Source characteristics of some foreshocks and aftershocks of Oct. 20, 1991 Uttarkashi earthquake *vis-a-vis* the Himalayan earthquakes", Memoir Geological Society of India, **30**, 51-64.

Gibowicz, S. B., 1973, "Stress drop and aftershocks", *Bull. Seismol. Soc. Am.*, **63**, 1433-1446.

Kanamori, K. and Anderson, D. L., 1975, "Theoretical basis of some empirical relations in Seismology", *Bull. Seismol. Soc. Am.*, **65**, 1073-1095.

Karnik, V., 1965, "Magnitude—Intensity relations for European and Mediterranean seismic regions," *Stud. Geophy. et. Geodaet. (Prague)*, **9**, 236-249.

Kayal, J. R., Kamble, V. P. and Rastogi, B. K., 1992, "Aftershock sequence of Uttarkashi earthquake of Oct. 20, 1991," Geological Survey of India, Special Publication No. 30, 203-217.

Narula, P. L. and Shome, S. K., 1992, "Macroseismic investigations of Uttarkashi earthquake of 20th Oct., 1991", Geological Survey of India, Special Publication No. 30, 1-165.

Press, F., 1975, "Earthquake Prediction," *Scientific American*, 232.

Rastogi, B. K., 1987, "Source mechanism of earthquakes in Himalaya and nearby regions", Proc. Indo-US Workshop on Earthquake Disaster Mitigation Research, DST, New Delhi, Vol. I-49 to IV-64.

Richter, C. F., 1958, Elementary Seismology, Freeman and Co., San Francisco.

Srivastava, H. N. and Kamble, V. P., 1972, "Aftershock characteristics in Himalayan mountain belt and neighbourhood", *Indian J. Met. Geophys.*, **23**, 75-82.

Utsu, T., 1961, "A statistical study on the occurrence of aftershocks", *Geophys. Mag.* (Tokyo), **30**, 521-605.